

# Detecting cold gas at intermediate redshifts: GMRT survey using Mg II systems.

Neeraj Gupta<sup>1</sup>, R. Srianand<sup>2</sup>, P. Petitjean<sup>3</sup>, P. Khare<sup>4</sup>, D. J. Saikia<sup>1</sup>, D. G. York<sup>5</sup>

## ABSTRACT

Intervening H I 21-cm absorption systems at  $z \geq 1.0$  are very rare and only 4 confirmed detections have been reported in the literature. Despite their scarcity, they provide interesting and unique insights into the physical conditions in the interstellar medium of high- $z$  galaxies. Moreover, they can provide independent constraints on the variation of fundamental constants. We report 3 new detections based on our ongoing Giant Metrewave Radio Telescope (GMRT) survey for 21-cm absorbers at  $1.10 \leq z_{\text{abs}} \leq 1.45$  from candidate damped Lyman- $\alpha$  systems. The 21-cm lines are narrow for the  $z_{\text{abs}} = 1.3710$  system towards SDSS J0108–0037 and  $z_{\text{abs}} = 1.1726$  system toward SDSS J2358–1020. Based on line full-width at half maximum, the kinetic temperatures are  $\leq 5200$  K and  $\leq 800$  K, respectively. The 21-cm absorption profile of the third system,  $z_{\text{abs}} = 1.1908$  system towards SDSS J0804+3012, is shallow, broad and complex, extending up to  $100 \text{ km s}^{-1}$ . The centroids of the 21-cm lines are found to be shifted with respect to the corresponding centroids of the metal lines derived from SDSS spectra. This may mean that the 21-cm absorption is not associated with the strongest metal line component.

*Subject headings:* cosmology: quasars: absorption lines–radio lines:galaxies

## 1. Introduction

The diffuse interstellar medium exhibits a wide range of physical conditions such as temperature, density and radiation field that are influenced by in-situ star-formation, cosmic

---

<sup>1</sup>NCRA, Postbag 3, Ganeshkhind, Pune 411007, India; neeraj@ncra.tifr.res.in; djs@ncra.tifr.res.in

<sup>2</sup>IUCAA, Postbag 4, Ganeshkhind, Pune 411007, India; anand@iucaa.ernet.in

<sup>3</sup>Institut d’Astrophysique de Paris – CNRS, 98bis Boulevard Arago, F-75014 Paris, France; ppetitje@iap.fr

<sup>4</sup>Department of Physics, Utkal University, Bhubaneswar 751004, India; khare@iopb.res.in

<sup>5</sup>Department of Astronomy & Astrophysics and Enrico Fermi Institute, 5640 S. Ellis Avenue, Univ. of Chicago, Chicago, IL 60637; don@oddjob.uchicago.edu

ray energy density, photoelectric heating by dust as well as mechanical energy input from both impulsive disturbances such as supernova explosions and steady injection of energy in the form of stellar winds. Therefore, understanding the physical conditions in the gas and the processes that maintain these is important for understanding galaxies and their evolution. The damped Lyman- $\alpha$  systems (DLAs), with  $\log N(\text{H I}) \geq 20.3$ , are a major reservoir of H I at high  $z$  and possibly the progenitors of present-day galaxies (see Wolfe et al. 2005). At high  $z$ , despite many attempts, only a handful of DLA galaxies have been detected based on line and/or continuum emission (see Møller et al. 2004).

Our understanding of physical conditions in DLAs at  $z \geq 1.8$  is based primarily on the absorption lines of  $\text{H}_2$  molecules and atomic fine-structure lines. A systematic search for  $\text{H}_2$  in DLAs at ( $z_{\text{abs}} > 1.8$ ) has resulted in a detection in  $\sim 15\%$  of the cases (see Ledoux et al. 2003). Usually, the DLAs with  $\text{H}_2$  absorption also show absorption lines of C I, C I\*, C I\*\* and C II\*. Detailed investigations show that  $\text{H}_2$  components have properties similar to that of the cold neutral medium (CNM) in a radiation field of moderate intensity originating from local star formation activity (Srianand et al. 2005). Using C II\* absorption lines Wolfe et al. (2004) have concluded that most of the DLAs at high  $z$  consist of CNM gas. However, above techniques cannot be used to probe nature of the gas at low and intermediate redshifts. In this case detecting 21-cm absorption line is one complementary way to probe the nature of absorbing gas. There have been several systematic searches for 21-cm absorption in DLAs undertaken by various groups (Briggs & Wolfe 1983; Lane 2000; Kanekar & Chengalur 2003, Curran et al. 2005) with limited success. To date, in the literature 38 DLAs have been searched for 21-cm absorption, resulting in 17 detections most of which occur  $z < 1$  (see Fig. 1). The column density of H I for an optically thin cloud that covers a fraction  $f_c$  of the background source is related to the optical depth  $\tau(v)$  in a velocity interval  $v$  and  $v+dv$  and to the spin temperature ( $T_s$ ) by

$$N(\text{H I}) = 1.835 \times 10^{18} \frac{T_s}{f_c} \int \tau(v) dv \text{ cm}^{-2}. \quad (1)$$

The low detection rate at high  $z$  can therefore be attributed either to the gas being warm (high  $T_s$ ) or to a low value of the covering factor ( $f_c$ ) through high  $z$  geometry effects (see Kanekar & Chengalur, 2003 and Curran & Webb, 2006, respectively). However, the redshift coverage is sparse and measurements are available only for a few systems at  $1 \leq z \leq 2$  (Fig. 1). To improve the statistics we have started a systematic survey of 21-cm absorption at  $1.10 \leq z \leq 1.45$  using the 610-MHz receiver at GMRT. Here, we report the results from the first phase of this survey that has resulted in 3 new detections.

Obtaining a new DLA sample at  $z \leq 1.6$  is virtually impossible in the absence of UV-spectrographs in space as the redshifted wavelength of Lyman- $\alpha$  line falls below the atmospheric cutoff. However, Rao & Turnshek (2000) have shown that the DLAs can be prese-

lected on the basis of equivalent widths of Mg II, Fe II and Mg I absorption lines. Specifically, they found that 50% of the absorbers with rest frame  $W(\text{Fe II}\lambda 2600)$  and  $W(\text{Mg II}\lambda 2796)$  greater than  $0.5 \text{ \AA}$  were confirmed DLAs. The detection rate becomes 100% when  $W(\text{Mg I}) \geq 0.5 \text{ \AA}$ . It is also clear from Fig. 3.4 of Lane (2000) that such a selection will also ensure that 50% of these candidates are detected in 21-cm absorption. Motivated by this, we have begun a GMRT 21-cm survey of DLA candidates selected on the basis of  $W(\text{Mg II})$  in the redshift range  $1.10 \leq z \leq 1.45$ . Our complete sample is drawn from the catalog of 7421 Mg II systems with  $W(\text{Mg II}) \geq 1 \text{ \AA}$  and  $0.3 \leq z \leq 1.9$ , detected along the line of sight toward 45,023 QSOs in SDSS DR3 (Prochter, Prochaska & Burles, 2006). There are 2857 systems at  $1.10 \leq z \leq 1.45$ . Out of these, we have selected all the 26 systems that have an estimated 610 MHz flux density in excess of 100 mJy from NVSS and First catalog. These form our main sample. In addition to this we have also observed three other sources [J0108–0037 (York et al. 2006), J0240–2309 and J1604–0019 (Lanzetta, Wolfe & Turnshek, 1987)] that have total flux density at 610 MHz in excess of 1 Jy and have strong Mg II systems.

## 2. Observations and Results

In the first phase of our GMRT survey we have observed 10 systems (Table 1) from our sample. Usually, a 1 MHz bandwidth split into 128 frequency channels was used to acquire data in the two circular polarization channels RR and LL. Broader (2 MHz for J0804+3012) or narrower (0.5 MHz for J2358–1020) bandwidths were used in the subsequent observing runs that were carried out for confirming the detected absorption. The data were reduced using the Astronomical Image Processing System (NRAO AIPS package) following standard procedures as described in Gupta et al. (2006). Final spectra for the three new detections and six non-detections are presented in Figs. 2 and 3 respectively. Analysis of  $z_{\text{abs}} = 1.3647$  towards J0240–2309 is presented in Srianand, Gupta & Petitjean (2006). In most of the cases the background quasar is unresolved for the typical  $5'' \times 5''$  synthesized beam achieved in our observations. However, for J0804+3012, J1411–0300 and J1604–0019 the radio sources are extended (see Fig. 4). For J0804+3012, 21-cm absorption is detected in the spectrum extracted towards the radio peak (Fig. 2). Higher spatial resolution as well as S/N observations will be required to investigate its variation across the source. In the case of J1411–0300, the radio peak is not consistent with the location of the optical source. 21-cm absorption is not detected towards either the strongest radio peak (P1) or another peak (P2) northeast to P1 (Figs. 3 and 4). No 21-cm absorption is detected towards any of the three prominent radio peaks seen in J1604–0019. Fig. 3 shows the spectrum towards the central component. A narrow absorption is present with  $\tau_{\text{peak}} \sim 0.04 \pm 0.01$  and  $\text{FWHM} = 6.1 \pm 2.3 \text{ km s}^{-1}$  near the expected frequency towards J0845+4257 (see Fig. 3). The feature is present

in both the polarizations and in the spectra extracted using different baselines and time ranges. At this stage we consider this as a tentative detection.

### 2.1. $z_{\text{abs}}=1.3710$ system towards J0108–0037

The 21-cm absorption profile is well fitted with a single Gaussian having  $\tau_{\text{peak}} = 0.068 \pm 0.002$  and  $\text{FWHM} = 15.4 \pm 0.6 \text{ km s}^{-1}$ . From the observed optical depth we get the integrated column density,  $N(\text{H I}) = 2.1 \times 10^{18} (T_s/f_c) \text{ cm}^{-2}$ . High frequency VLBA observations suggest structures extending over 60 mas ( $\sim 50 \text{ pc}$ ;  $H_0=71 \text{ km s}^{-1} \text{ Mpc}^{-1}$ ,  $\Omega_m=0.27$ ,  $\Omega_\Lambda=0.73$ ) with significant flux density in extended emission (Beasley et al. 2002). Thus  $f_c$  is uncertain. Assuming thermal broadening, gives a gas kinetic temperature  $T_K = 21.86 \times (\frac{\text{FWHM}}{\text{km s}^{-1}})^2 \leq 5200 \text{ K}$ . This is an upper limit as various other effects also could contribute to the line width. Now we can assume  $T_s = T_K$  as is the case for thermodynamic equilibrium. If the gas is a typical CNM (say  $T_s = T_K = 100 \text{ K}$ ) then  $\log [f_c N(\text{H I})] = 20.30$ . Thus,  $N(\text{H I})$  in the 21-cm component is consistent with it being a DLA. The 21-cm centroid is within  $4 \text{ km s}^{-1}$  to that expected from the metal lines detected in the SDSS spectrum. The Zn II+Cr II blend at  $\lambda = 2062 \text{ \AA}$ , the Si II  $\lambda 1808$  and the Mn II lines are clearly detected even in the low-dispersion SDSS spectrum.

### 2.2. $z_{\text{abs}}=1.1908$ system towards J0804+3012

21-cm absorption is clearly detected towards J0804+3012 which is partially resolved in our observations (Fig. 4). The absorption profile is consistent with a main component (with  $\text{FWHM} \sim 44 \pm 19 \text{ km s}^{-1}$  and  $\tau_{\text{peak}} = 0.006 \pm 0.001$ ) and a broad wing (extending up to  $\sim 100 \text{ km s}^{-1}$ ) towards higher frequency. Our two-epoch observations with different spectral resolution confirm the main component which also shows the expected Doppler shift. However, deeper observations are required to ascertain the strength of the wing. It is interesting to note that the expected position of 21-cm absorption based on the SDSS spectrum coincides with the wing of the 21-cm absorption and not the stronger main component. Based on the profile obtained on 15–16 September 2006, we get an integrated column density of  $N(\text{H I})=6.5 \times 10^{17} (T_s/f_c) \text{ cm}^{-2}$ . Unlike the other two 21-cm absorbers, we do not detect Si II  $\lambda 1808$  (with  $W \leq 0.3 \text{ \AA}$ ) and Zn II  $\lambda 2026$  lines (with  $W \leq 0.2 \text{ \AA}$ ) in the SDSS spectrum.

### 2.3. $z_{\text{abs}}=1.1726$ system towards J2358–1020

Relatively weak 21-cm absorption is clearly detected and the profile can be well fitted with a single Gaussian component with  $\tau_{\text{peak}} = 0.035 \pm 0.004$  and  $\text{FWHM} = 6.0 \pm 0.8$  km s<sup>-1</sup> (Fig 2). This implies  $T_{\text{k}} \leq 800$  K and  $\log [f_c N(\text{H I})] \leq 20.5$  in the 21-cm absorbing component. If the absorbing gas happens to be a CNM then  $\log [f_c N(\text{H I})] = 19.6$ . The value of  $f_c$  could be close to unity as VLBA observations at 5 GHz by Fomalont et al. (2000) show the source to be  $\leq 0.5$  mas, which corresponds to a projected size of  $\leq 4$  pc at  $z_{\text{abs}}=1.1726$ . Thus the inferred range in  $N(\text{H I})$  is consistent with the 21-cm absorbing gas being a sub-DLA. Like the previous system, the 21-cm absorption is shifted by 70 km s<sup>-1</sup> with respect to the optical redshift based on the SDSS data. The Zn II+Cr II blend at  $\lambda = 2062$  Å is clearly detected in the SDSS spectrum. The compactness of the background radio source and the simplicity of the 21-cm absorption profile make this system an ideal case for probing the variation of fundamental constants.

## 3. Discussion

In this letter we have reported the detection of 21-cm absorption in three systems. This has substantially increased the number of 21-cm absorption systems at  $z > 1.0$ , as prior to this only four systems were known. In two of our systems ( $z_{\text{abs}} = 1.1908$  towards J0804+3012 and  $z_{\text{abs}} = 1.1726$  towards J2358–1020) the centroid of the strongest 21-cm absorption component is shifted with respect to the centroid of metal lines derived from SDSS spectra. This may mean that the strongest 21-cm absorption component is not associated with the strongest metal absorption component. Such shifts have already been observed in other systems (see Srianand et al. 2005; Kanekar et al. 2006; Heinmüller et al. 2006). It is also known that H<sub>2</sub> carrying components in DLAs, that are believed to trace the CNM gas, often show similar shifts (although less pronounced) with respect to the strong metal line components (Ledoux et al. 2003). H<sub>2</sub> components often distinguish themselves with respect to the rest of the velocity components by the presence of excited fine-structure lines of C I and C II and in some cases by large depletion factors (e.g. Rodríguez et al. 2006). It would be very important to obtain high resolution optical spectra of our sources to see if this is also true in the case of the 21-cm absorption systems.

We also report upper limits on 7 systems with one of them being a tentative detection. We find a detection rate of 21-cm absorption of roughly 30% in our survey so far. This is much higher than that achieved earlier (see for example Lane, 2000), mainly because we have restricted ourselves to the stronger Mg II systems. Since the objects observed during the first-phase of the survey are drawn randomly from the parent sample, most probably the

detection rate of our whole survey will be close to what we have achieved so far. In Fig. 5 we compare the properties of our systems with those of DLAs in the sample of Rao & Turnshek (2000). The distribution of different equivalent width ratios together with the distribution of  $W(\text{Mg II})$  in our sample is consistent with what is observed in the DLA population.

It is important to obtain independent constraints on the time variation of fundamental constants in order to resolve the controversy regarding the variation of  $\alpha$  (Murphy et al. 2003; Srianand et al. 2004). As the energy of the 21-cm transition depends on the electron-to-proton mass ratio ( $\mu$ ), the fine-structure constant ( $\alpha$ ) and the proton G-factor ( $G_p$ ), high resolution optical spectra in conjunction with high resolution 21-cm spectra can be used to probe the variation of these constants (Tzanavaris et al. 2005). However, it is important first to understand the origin of the relative shifts that we observe between the redshifts of the atomic heavy element lines and the 21-cm absorption. This needs detailed modeling of the absorption systems taking into account all transitions simultaneously. This is what we plan to do in the near future.

RS and PPJ gratefully acknowledge support from the Indo-French Centre for the Promotion of Advanced Research (IFCPAR) under contract No. 3004-3. We thank the referee for useful comments, Rajaram Nityananda for encouragement and GMRT staff for their co-operation during observations. The GMRT facility is run by NCRA-TIFR.

## REFERENCES

- Beasley, A. J., Gordon, D., Peck, A. B., Petrov, L., MacMillan, D. S., Fomalont, E. B., & Ma, C., 2002, *ApJS*, 141, 13
- Briggs, F. H., & Wolfe, A.M., 1983, *ApJ*, 268, 76
- Curran, S.J., Murphy, M. T., Pihlström, V. M., Webb, J. K, & Purcell, C. R. 2005, *MNRAS*, 356, 1509
- Curran, S. J., & Webb, J. 2006, *MNRAS*, 371, 356.
- Fomalont, E. B., Frey, S., Paragi, Z., Gurvits, L. I., Scott, W. K., Taylor, A. R., Edward, P. G., & Hirabayashi, H, 2000, *ApJS*, 131, 95
- Gupta, N., Salter, C.J., Saikia, D.J., Ghosh, T., & Jeyakumar, S., 2006, *MNRAS*, in press (astro-ph/0605423)
- Heinmüller, J., Petitjean, P., Ledoux, C., Caucci, S., & Srianand, R., 2006, *A&A*, 449, 33

- Kanekar, N., & Chengalur, J.N., 2003, *A&A*, 399, 857
- Kanekar, N., Subrahmanyam, R., Ellison, S.L., Lane, W.M., & Chengalur, J.N., 2006, *MNRAS*, 370, L46
- Lane W., 2000, PhD Thesis, University of Groningen
- Lanzetta, K. M., Wolfe, A. M., & Turnshek, D. A, 1987, *ApJ*, 322, 739
- Ledoux, C., Petitjean, P., & Srianand, R., 2003, *MNRAS*, 346, 209
- Möller, P., Fynbo, J. P. U., & Fall, S. M., 2004, *A&A*, 422, 33
- Murphy, M. T., Webb, J. K., & Flambaum, V. V., 2003, *MNRAS*, 345, 609
- Prochter, G. E., Prochaska, J. X., Burles, S. M., 2006, *ApJ*, 639, 766
- Rao, S.M., Turnshek, D.A., 2000, *ApJS*, 130, 1
- Rodríguez, E., Petitjean, P., Aracil, B., Ledoux, C., & Srianand, R. 2006, *A&A*, 446, 791
- Srianand, R., Chand, H., Petitjean, P., & Aracil, B, 2004, *PRL*, 92, 121302
- Srianand, R., Gupta, N., & Petitjean, P., 2006, *MNRAS*, in press (astro-ph/0611327)
- Srianand, R., Petitjean, P., Ledoux, C., Ferland, G., & Shaw, G., 2005, *MNRAS*, 362, 549
- Tzanavaris, P., Webb, J. K., Murphy, M. T., Flambaum, V. V., & Curran, S. J., 2005, *PRL*, 95, 1301
- Wolfe, A.M., Howk, J.C., Gawiser, E., Prochaska, J.X., & Lopez, S., 2004, *ApJ*, 615, 625
- Wolfe, A.M., Gawiser, E., Prochaska, J.X., 2005, *ARA&A*, 43, 861
- York, D. G., et al. 2006, *MNRAS*, 367, 945.

Table 1: Observational log and results.

Name	$z_{\text{abs}}$	Time (hr)	Peak flux <sup>a</sup>	rms <sup>b</sup>	$\tau^c$
J0108–0037	1.3710	4.4	1276	2.9	0.070
J0214+1405	1.4463	4.4	220	2.7	<0.012
J0240–2309	1.3647	8.0	5100	5.2	<0.001
J0748+3006	1.4470	5.5	347	3.5	<0.010
J0804+3012	1.1908	6.0	2050	1.9	0.006
		6.2 <sup>d</sup>	2087	1.6	0.006
J0845+4257	1.1147	5.0	224	3.0	<0.013
J1017+5356	1.3055	4.4	127	2.3	<0.018
J1411–0300 <sup>e</sup>	1.4160	3.9	244	3.0	<0.012
			161	3.0	<0.019
J1604–0019	1.3245	3.3 <sup>d,f</sup>	375	3.9	<0.010
J2358–1020	1.1726	3.9 <sup>d,f</sup>	443	1.4	0.033
		5.5 <sup>g</sup>	420	2.5	0.035

<sup>a</sup> peak flux (mJy/beam); <sup>b</sup> spectral rms (mJy/beam/channel)

<sup>c</sup> peak optical depth or 1- $\sigma$  limit per channel;

<sup>d</sup> 2 MHz band width.

<sup>e</sup> The two spectra correspond to peaks P<sub>1</sub> and P<sub>2</sub>.

<sup>f</sup> 256 channels used; <sup>g</sup> 0.5 MHz bandwidth



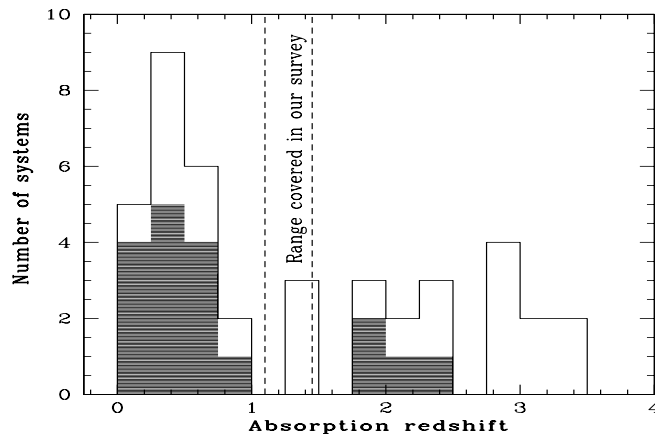


Fig. 1.— Line-histogram is the redshift distribution of the DLAs for which redshifted 21-cm observations are reported (Table. 1 of Curran et al. 2005 and  $z = 2.347$  towards PKS 0438–436 from Kanekar et al. 2006). Shaded histogram is for the confirmed 21-cm absorption systems. The redshift range covered in our GMRT survey is also marked.

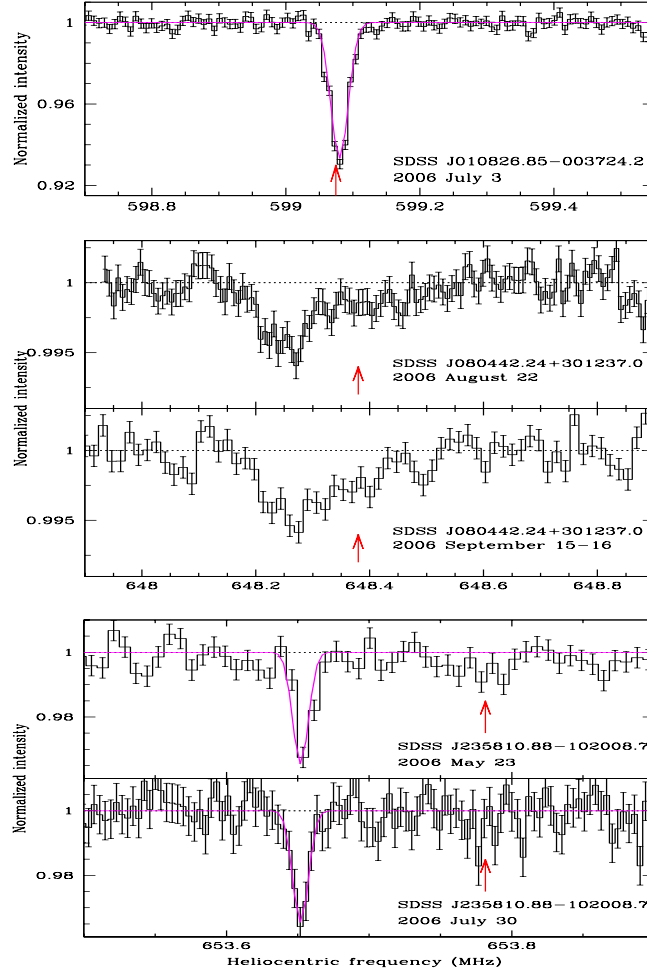


Fig. 2.— GMRT H I spectra of the sources with 21-cm absorption. Single Gaussian fits are overplotted in the case of J0108–0037 and J2358–1020. Arrows mark the expected positions of 21-cm absorption based on the metal absorption lines.

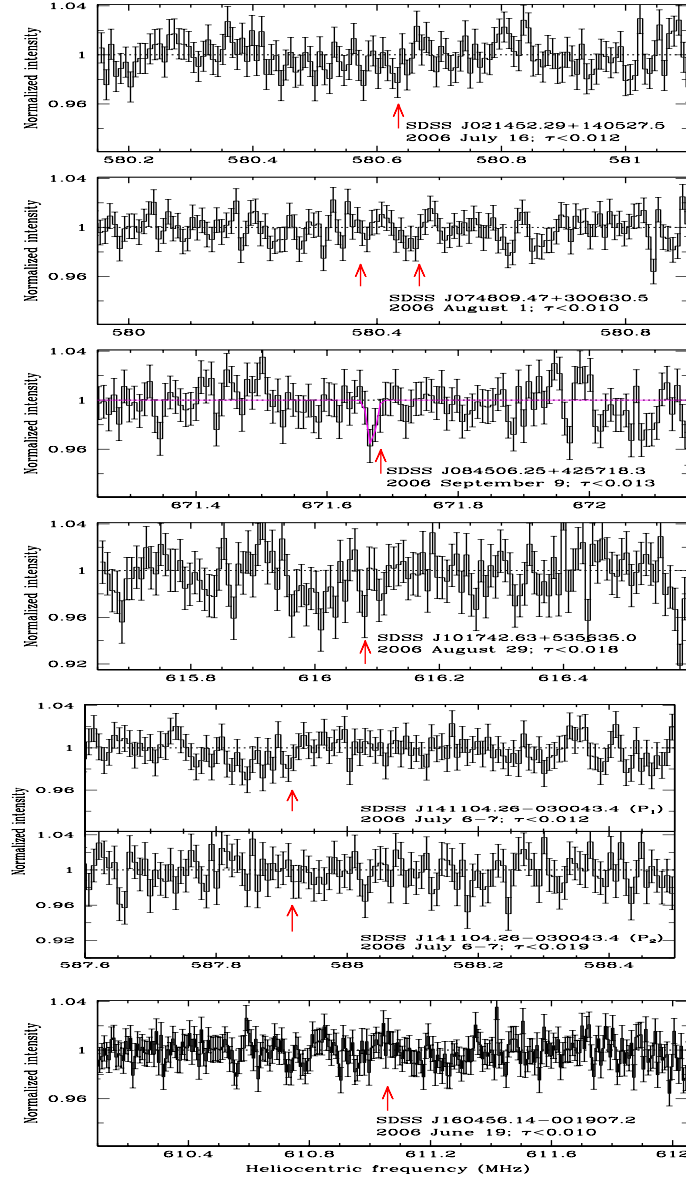


Fig. 3.— Spectra for the sources with non-detection in 21-cm absorption. Arrows mark the expected position of 21-cm absorption based on the metal absorption lines.

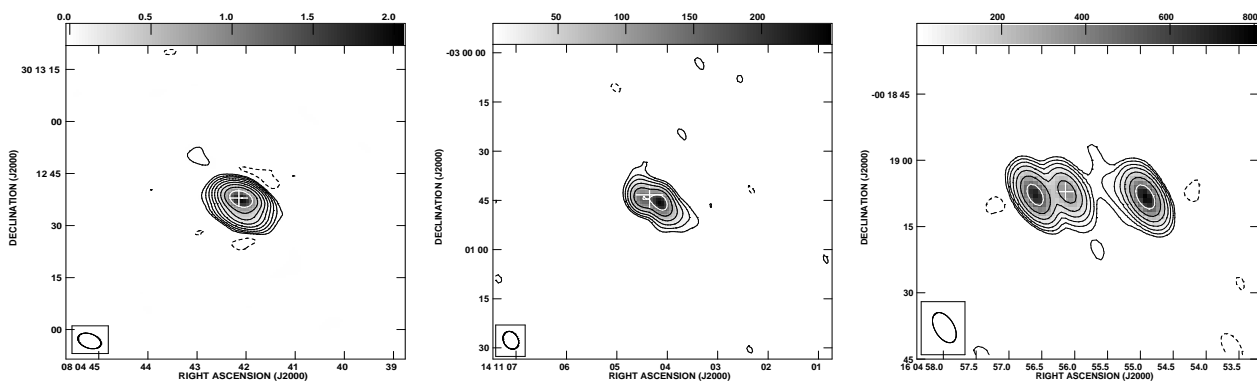


Fig. 4.— GMRT maps of sources resolved in our observations with contour levels as  $n \times (-1, 1, 2, 4, \dots)$  mJy/beam. **(a)** J0804+3012 with an rms of 0.84 mJy/beam and beam of  $6.36'' \times 4.09''$  with position angle (PA) =  $67^\circ$  and  $n=4$ . **(b)** J1411-0300 with an rms of 1.25 mJy/beam and beam of  $5.67'' \times 4.32''$  with PA =  $28^\circ$  and  $n=5$ . **(c)** SDSS J1604-0019 with an rms of 1.50 mJy/beam and beam of  $7.55'' \times 4.34''$  with PA =  $32^\circ$  and  $n=8$ . The position of the optical source in each image is marked as a cross.

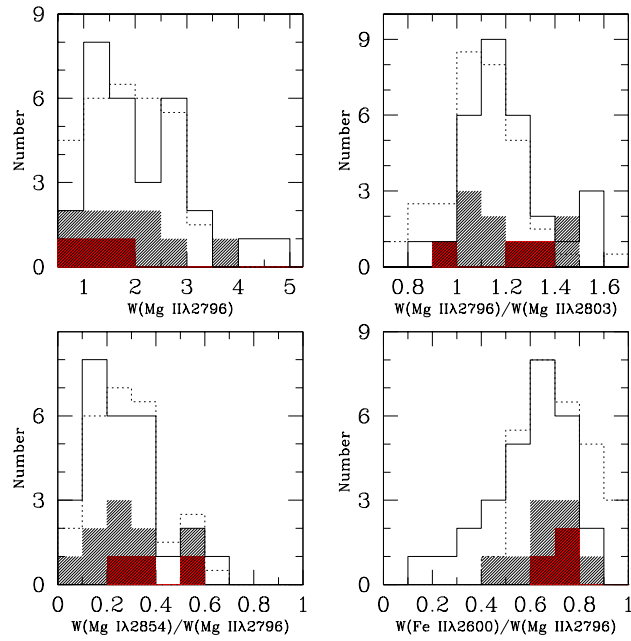


Fig. 5.— Distributions of  $W(\text{Mg II})$  and different line ratios. Solid and dotted histograms are respectively for our GMRT sample and the sample of DLAs (downscaled by factor 2) studied by Rao & Turnshek (2000). Light and dark histograms are for the systems observed for 21-cm absorption so far and the systems with detections respectively.